

Technical Memorandum

To: Jeff Uhlmeyer

From: Lauren Gardner, Gonzalo Rada, and Kevin Senn

cc: Mustafa Mohamedali

Date: September 3, 2020 (Original); November 20, 2020 (Revised)

Re. Forensic Desktop Study Report: Utah LTPP Test Sections 49_7082, 49_7085, and 49_7086

The Long-Term Pavement Performance GPS-3 Jointed Plain Concrete Pavement (JPCP) test sections 49_7082, 49_7085, and 49_7086¹ were nominated for a desktop study under TPF-5(332) "LTPP Forensic Evaluations." The test sections were incorporated into the LTPP program in the 1990 to 1991 time period with similar pavement structures (undoweled JPCP), but have different climatic factors and traffic characteristics. The purpose of this investigation is to compare the performance of these test sections to each other, and to identify those factors driving the differences in the performance of the measures.

SITE DESCRIPTIONS

All three projects are located near Salt Lake City. LTPP test section 49_7082 is located on Interstate 15, northbound, in Box Elder County, Utah. Interstate 15 is a rural principal arterial-interstate with two lanes in the direction of traffic. LTPP test section 49_7085 is located on U.S. 40, eastbound, in Wasatch County, Utah. U.S. 40 is a rural principal arterial with two lanes in the direction of traffic. LTPP test section 49_7086 is located on State Route 154, southbound in Salt Lake County, Utah. State Route 154 is an urban principal arterial with three lanes in the direction of traffic. All three test sections are classified as being in a Dry, Freeze climate zone. The coordinates (in degrees) of the test sections 49_7082, 49_7085, and 49_7086 are 41.84543, -112.17366, 40.56577, -111.42923, and 40.71588, -111.98435, respectively. Photographs 1 through 3 show the three test sections at Station 0+00 looking northbound (49_7082), eastbound (49_7085), and southbound (49_7086) in 2015, while Map 1 shows the geographical location of the test sections.

¹ First two digits in test section number represent the State Code [49 =Utah]. The final four digits are unique within each State/Province and were assigned at the time the test section was accepted into the LTPP program.



Photograph 1. LTPP Section 49_7082 at Station 0+00 looking northbound in 2015.



Photograph 2. LTPP Section 49_7085 at Station 0+00 looking eastbound in 2015.



Photograph 3. LTPP Section 49_7086 at Station 0+00 looking southbound in 2015.



Map 1. Geographical location of test sections.

BASELINE PAVEMENT HISTORY

This section of the document presents historical data on the pavement structures and their structural capacity, climate, traffic, and pavement distresses.

Pavement Structure and Construction History

Test section 49_7082² was accepted into the LTPP Program as part of the GPS-3 experiment in October 1989 with the knowledge it would officially start being monitored following the planned reconstruction completed in November 1990. The pavement structure after reconstruction consisted of 9.8 inches of Portland Cement Concrete (PCC), 4.2 inches of lean concrete base, 4 inches of crushed gravel unbound granular subbase, 18 inches of unbound soil-aggregate mixture granular subbase, and a clayey gravel with sand subgrade. This pavement structure is summarized in Table 1; this information corresponds to CONSTRUCTION_NO = 1 (CN = 1) in the LTPP database. The next construction event occurred in June 2013, when the surface was diamond grinded, and joint load transfer was restored. This construction event (CN=2) did not affect the overall pavement structure summarized in Table 1.

Table 1. Pavement structure for 49_7082 (CN=1 and CN=2)

Layer Number	Layer Type	Thickness (in.)	Material Code Description
1	Subgrade (untreated)		Coarse-Grained Soil: Clayey Gravel with Sand
2	Unbound (granular) subbase	18	Soil-Aggregate Mixture (Predominantly Coarse-Grained)
3	Unbound (granular) subbase	4	Crushed Gravel
4	Bound (treated) base	4.2	Lean Concrete
5	Portland cement concrete layer	9.8	Portland Cement Concrete (JPCP)

Test section 49_7085 was accepted into the LTPP Program as part of the GPS-3 experiment in June 1991 with the knowledge it would officially start being monitored following the planned reconstruction completed in in October 1991. The pavement structure after reconstruction consisted of 9.7 inches of PCC, 4.8 inches of lean concrete base, 4 inches of crushed gravel unbound granular subbase, 18 inches of unbound soil-aggregate mixture granular subbase, and a silty gravel with sand subgrade. This pavement structure is summarized in Table 2; this information corresponds to CONSTRUCTION_NO = 1 (CN = 1) in the LTPP database. The next construction event occurred in June 2001, when the section received crack sealing, transverse joint sealing, and lane shoulder longitudinal joint sealing (CN=2). A third construction event (CN=3) occurred in 2012, when the section received additional crack sealing and transverse joint sealing, the surface was diamond grinded, joint load transfer restored, and there was a replacement of some of the PCC slabs. Neither CN=2 nor CN=3 changed the pavement structure of the test section summarized in Table 2. The section was subsequently taken out of study in May 2017.

Test section 49_7086² was accepted into the LTPP Program as part of the GPS-3 experiment in June 1991 with the knowledge it would officially start being monitored following the planned reconstruction completed in in October 1991. The pavement structure after reconstruction consisted of 10.1 inches of PCC, 5.4 inches of lean concrete base, 16 inches of unbound soil-aggregate mixture granular subbase (over two layers), 0.5-inch non-woven geotextile, 12 inches of crushed gravel unbound granular subbase, 0.1-inch woven geotextile, and a clayey gravel with sand subgrade. This pavement structure is summarized in Table 3; this information corresponds to CONSTRUCTION_NO = 1 (CN = 1) in the LTPP database. The next construction event occurred in May 2001, when the section received transverse joint sealing and lane shoulder longitudinal joint sealing (CN=2). A third construction event (CN=3) occurred in 2010, when the

² Please note that according to LTPP InfoPave, these sections went out of study in January 2020. However, this information is not correct as the sites are still active.

section received surface grinding and partial depth patching. A final event (CN=4) occurred in 2013, when the test section surface was diamond grinded and additional transverse joint sealing occurred. CN=2, CN=3, and CN=4 did not change the pavement structure of the test section summarized in Table 3.

Table 2. Pavement structure for 49_7085 (CN=1, CN=2, and CN=3)

Layer Number	Layer Type	Thickness (in.)	Material Code Description
1	Subgrade (untreated)		Coarse-Grained Soil: Silty Gravel with Sand
2	Unbound (granular) subbase	18	Soil-Aggregate Mixture (Predominantly Coarse-Grained)
3	Unbound (granular) subbase	4	Crushed Gravel
4	Bound (treated) base	4.2	Lean Concrete
5	Portland cement concrete layer	9.8	Portland Cement Concrete (JPCP)

Table 3. Pavement structure for test section 49_7086 (CN=1, CN=2, CN=3, and CN=4)

Layer Number	Layer Type	Thickness (in.)	Material Code Description
1	Subgrade (untreated)		Coarse-Grained Soil: Clayey Gravel with Sand
2	Engineering Fabric	0.1	Woven Geotextile
3	Unbound (granular) subbase	12	Crushed Gravel
4	Engineering Fabric	0.5	Nonwoven Geotextile
5	Unbound (granular) subbase	12	Soil-Aggregate Mixture (Predominantly Coarse-Grained)
6	Unbound (granular) subbase	4	Soil-Aggregate Mixture (Predominantly Coarse-Grained)
7	Bound (treated) base	5.4	Lean Concrete
8	Portland cement concrete layer	10.1	Portland Cement Concrete (JPCP)

Pavement Structural Properties

Figure 1 shows the average Falling Weight Deflectometer (FWD) deflection under the nominal 9,000-pound load plate over time for the three test sections. The deflection of the sensor located in the center of the load plate is a general indication of the total “strength” or response of all layers in the pavement structure to a vertically applied load. This deflection can be influenced by pavement temperature at the time of testing, precipitation, and moisture. As depicted in Figure 1, the deflections observed on the three sites are minimal. The deflections observed range from 1.4 to 7.7 mils. Overall, section 49-7082 showed the smallest deflections throughout the analysis period. Sections 49-7085 and 49-7086 reported similar deflections with 49-7085 reporting smaller deflections until 2002 and subsequently section 49-7086 reporting smaller deflections following 2002.

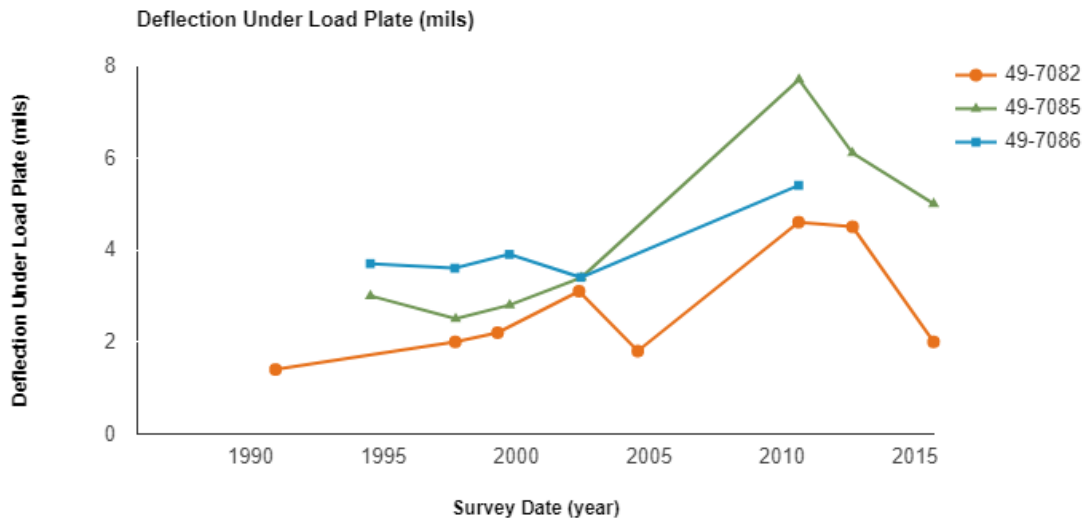


Figure 1. Time history of average deflection for the sensor located in the load plate normalized to 9,000 lb. drop load.

The layer moduli backcalculated from the deflection data were also assessed for the test sections. The pavement structure for test section 49-7082 was modeled as 9.8 inches of PCC, 4.2 inches of lean concrete base, and 22 inches of combination-coarse granular over coarse subgrade and bedrock. The pavement structure for test section 49-7085 was modeled as 9.7 inches of PCC, 4.8 inches of lean concrete base, and 22 inches of combination-coarse granular over coarse subgrade and bedrock. The pavement structure for test section 49-7086 was modeled as 10.1 inches of PCC, 5.4 inches of lean concrete base, and 28 inches of combination-coarse granular over coarse subgrade and bedrock. The modulus of the bedrock layer for all three test sections was assumed to be 500 ksi. The backcalculated moduli for each layer and section between December 1990 and August 2010 are shown in Figures 2 through 5.

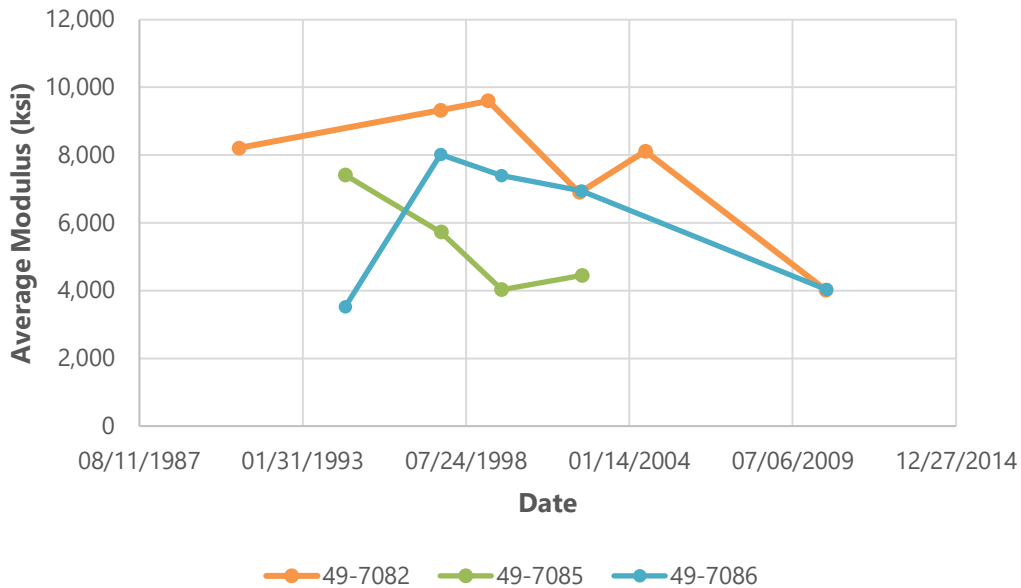


Figure 2. Average backcalculated modulus for portland cement concrete (Layer 1).

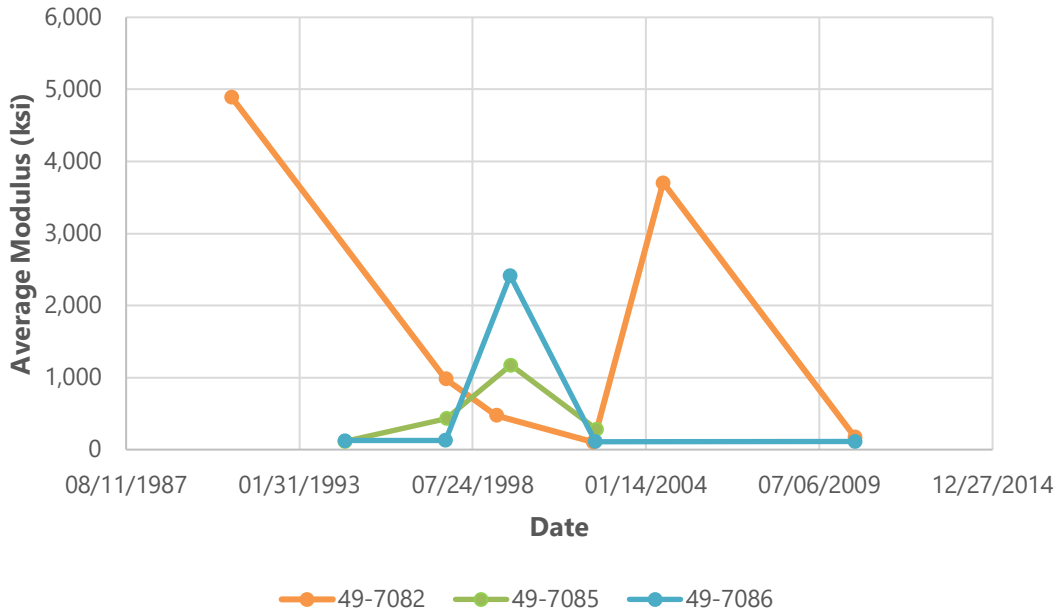


Figure 3. Average backcalculated modulus for lean concrete base (Layer 2).

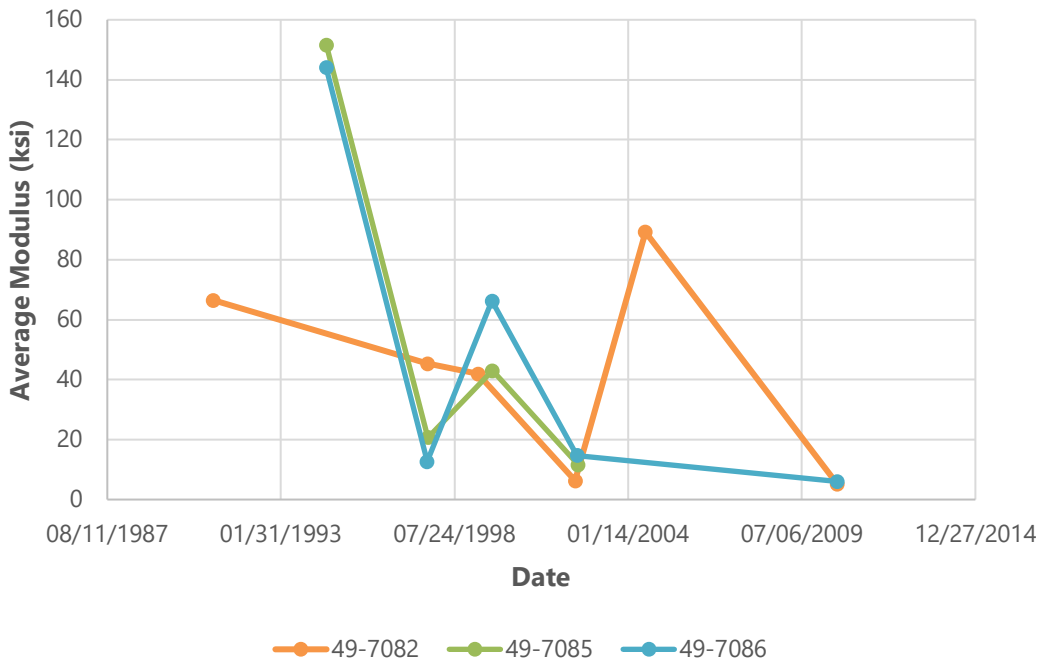


Figure 4. Average backcalculated modulus for combination - coarse granular subbase and typical granular subbase (Layer 3).

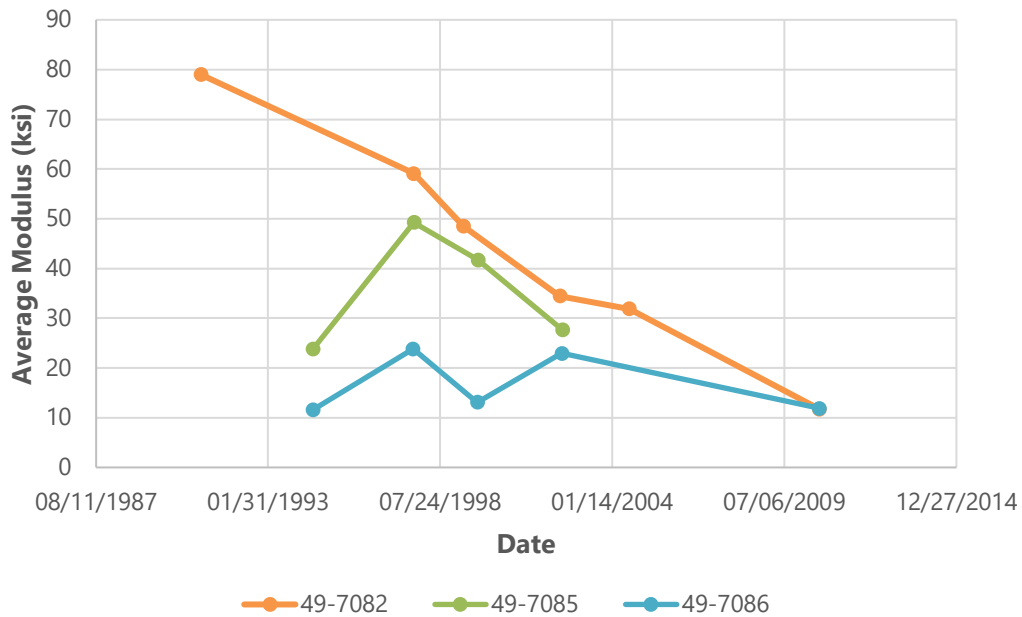


Figure 5. Average backcalculated modulus for coarse subgrade (Layer 4).

In general, the field-derived layer moduli appear reasonable for all four layers. Values for the PCC surface layer ranged between 3,500 and 8,000 ksi, which is a common range of PCC modulus values. The only exception was two points for test section 49_7082 with values in the 9,000 to 10,000 ksi range, which seem somewhat high and which may be the result of backcalculation analysis (e.g., compensating layer moduli, seed moduli values, etc.). Figure 2 also appears to indicate test sections 49_7082 has a slightly higher PCC modulus than test section 49_7086, which has a slightly higher PCC modulus than 49_7085.

The above conclusions about the reasonableness of the PCC backcalculated layer moduli is further confirmed by comparing the results to those derived from laboratory elastic modulus testing. Table 4 summarizes the laboratory test results for the PCC layer (lab results for the subgrade and base layers were limited). As shown, all laboratory test results fall within the range of 3,500 and 5,400 ksi, which is in line with the field-derived moduli (3,500 to 8,000 ksi).

Table 4. Comparison of lab and field results for the PCC layer

Test Section	Lab Results		Field Results	
	Number of Samples/test results	Range of moduli values (ksi)	Number of Samples/test results	Range of moduli values (ksi)
49_7082	1 sample (2 test results)	5,150 -5,400	6 test dates	4,013-9,598
49_7085	1 sample (2 test results)	3,650-4,100	4 test dates	4,027-7,409
49_7086	1 sample (2 test results)	3,950-4,100	5 test dates	3,523-8,021

The lean concrete base moduli ranged mostly between 100 and 1,100 ksi, which appears reasonable if the base layer has cracked, which would need to be confirmed. There are three points above 2,000 ksi, but as was the case with the PCC surface layer, it is suspected these higher values are related to the peculiarities of the backcalculation analysis. There is also no clear indication that the lean concrete base modulus is higher for one test section over the others.

In terms of the granular subbase and subgrade backcalculated layer moduli, the values range mostly between 6 and 65 ksi, which is quite reasonable for unbound granular material. There are three granular subbase values that exceed 80 ksi and one subgrade value that exceeds 60 ksi, but these appear to be related software backcalculation issues or due to ambient effects such as freezing of moisture in one or both of the unbound layers.

Climate History

The time history for average annual precipitation (from Modern-Era Retrospective analysis for Research and Applications or MERRA) since 1990 is shown in Figure 6. The mean precipitation recorded at sections 49_7082, 49_7085, and 49_7086 prior to 2019 was 19.6, 36.4, and 18.3 inches, respectively, for the period shown in Figure 6. For all three sites, the amount of precipitation reported spiked in 1996, 2010, 2017, and 2019. Section 49_7085 reported the highest amounts of precipitation overall, which is expected given its proximity to the mountainous Uinta-Wasatch-Cache National Forest. The precipitation observed on all three sites likely affected the performance of the test sections. This is especially the case of test section 49_7085, which has an average annual precipitation that is significantly higher than the other two test sections. Much or most of this precipitation is in the form of snow, and hence winter maintenance practices could play a factor in the performance of the test section. It is also worth noting the precipitation for test section 49_7085 falls outside the "Dry" definition (20 inches per year), so this will be brought to the attention of the LTPP program for correction.

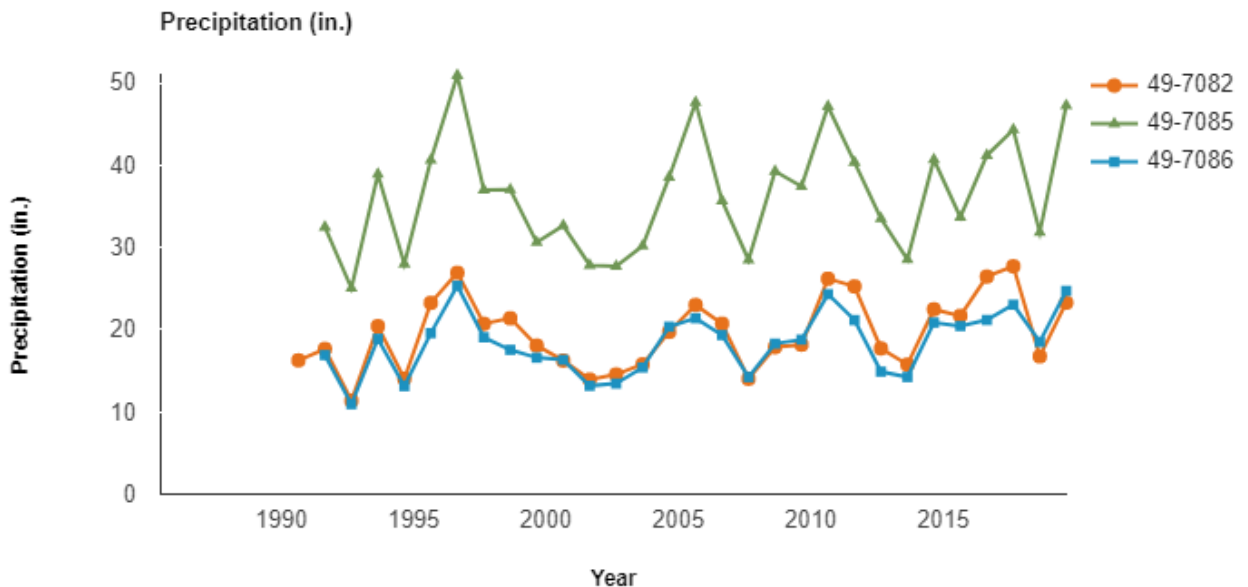


Figure 6. Average yearly precipitation over time.

Figure 7 shows the time history of the average annual freezing index (from MERRA) for the test sites. The freezing index is the summation of the difference between freezing temperature and the average air temperature when it is less than freezing over a year's time. This index is an indicator of the harshness of

the winter season relative to issues such as ground frost and low temperature cracking in pavements. As depicted in Figure 7, the freezing index values ranged from 621 (2003) to 1,413 deg F deg days (2008) for section 49_7082, from 1,004 (2014) to 2,196 deg F deg days (2008) for section 49_7085, and from 362 (2003) to 1,044 deg F deg days (2013) for section 49_7086—all of which are well above the 150 deg F deg days used to classify a freeze region. This indicates the freezing index is likely a factor affecting the performance of all the test sections. Additionally, while all three sections follow similar trends on a year to year basis, section 49_7085 reports noticeably higher freezing indices, followed by section 49_7082 and then section 49_7086. When viewed in combination with the annual precipitation history presented earlier, it appears that climate plays a more significant role on the performance of test section 49_7085 as compared to the other two test sections.

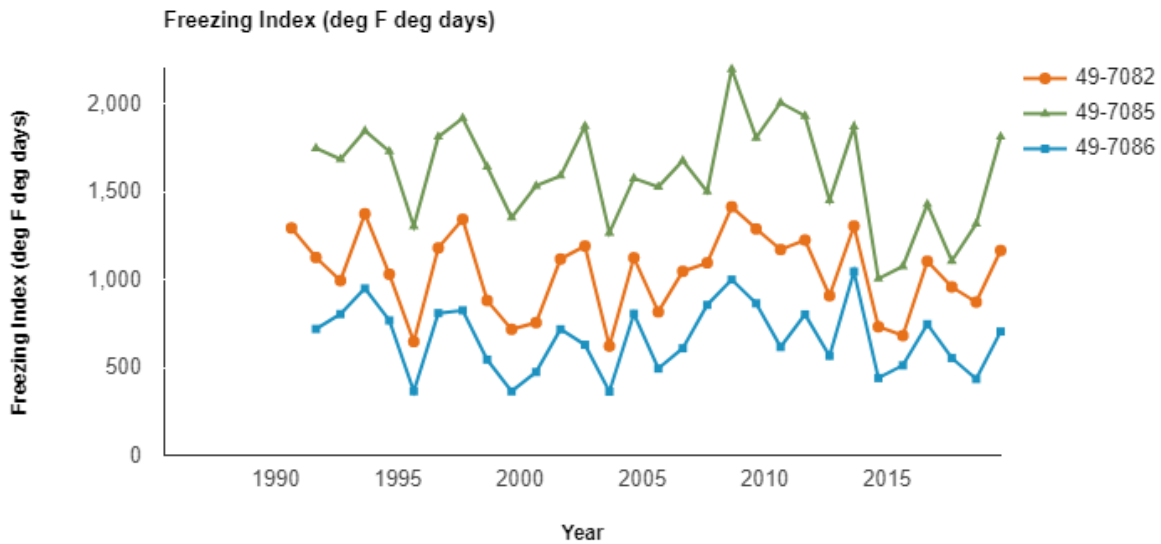


Figure 7. Average annual freezing index over time.

In addition to precipitation and freezing index information for the three sites, it is important to note the highest average annual temperature for the time period in question occurred at test section 49_7086 (48.4°F), followed by 49_7082 (44.8°F), and 49_7085 (39.5°F). Moreover, it is hypothesized these temperatures, like precipitation and freezing index, also affected the performance of the three test sections.

It is further noted that MERRA data were chosen for this desktop study over Virtual Weather Station (VWS) data also stored in the LTPP database because they are considered of higher quality, especially for mountainous terrain such as the one associated with the three test sections in question. The VWS precipitation generally agrees well with the MERRA precipitation data, but not so for the freezing index values, where the differences are not as pronounced as they are for the MERRA data. This issue will also be brought to the attention of the LTPP program.

Truck Volume History

Figure 8 shows the annual average daily truck traffic (AADTT) data in the LTPP test lane by year. For section 49_7082, the annual truck traffic counts increase from 273 in 1991 to 2,465 in 2017, or approximately 84 additional trucks per day per year. For section 49_7085, the annual truck traffic counts increase from 223 in 1992 to 909 in 2017, or approximately 27 additional trucks per day per year. For section 49_7086, the annual truck traffic counts increase from 448 in 1992 to 1,592 in 2017, or approximately 46 additional

trucks per day per year. The average number of ESALS reported on these sections also increased over time as depicted in Figure 9. For section 49_7082, the number of ESALS increased from 162,241 in 1991 to 1,466,698 in 2017. For section 49_7085, the number of ESALS increased from 98,824 in 1992 to 403,070 in 2017. For section 49_7086, the number of ESALS increased from 105,000 in 1992 to 352,349 in 2017. The fluctuations in both the AADTT and ESALS reported for the test sections is likely a result of the source of the data for each. A combination of state provided AADTT values, monitored values, values calculated using monitored class data, a compound growth function, or a linear growth function was used to report traffic along these test sections.

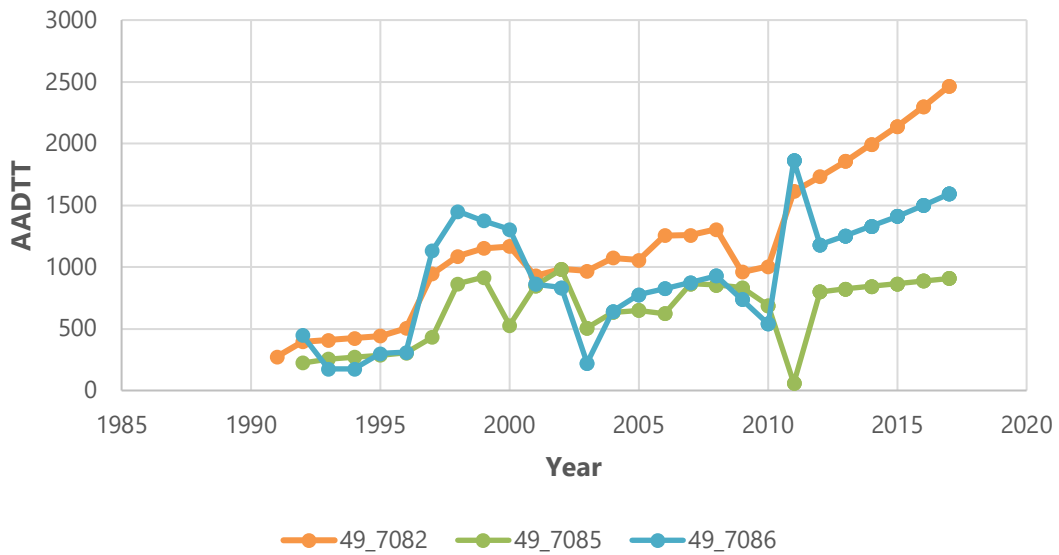


Figure 8. Average annual daily truck traffic (AADTT) history.

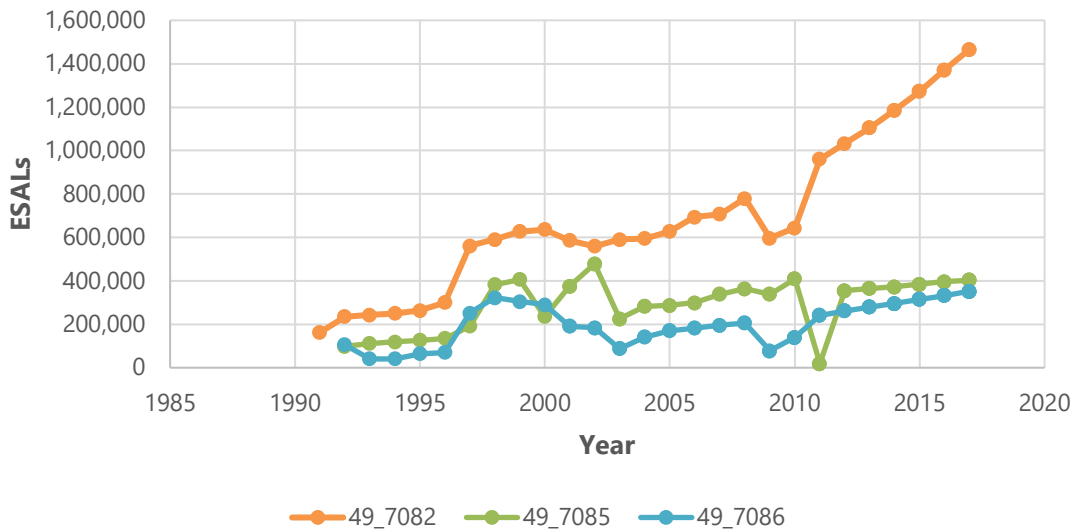


Figure 9. Estimated annual ESAL for vehicle classes 4-13 over time.

Pavement Distress History

The following section summarizes the distresses observed on the three test sections, two of which were last monitored in 2019, and the other was last monitored in 2015. Longitudinal cracking, transverse patching, corner breaks, IRI, faulting and wheelpath surface wear were assessed.

Longitudinal Cracking

Data on longitudinal cracking was collected between 1992 and 2019 as shown in Figures 10. The only section where longitudinal cracking is reported is 49_7085 which first reports 666 feet of cracking in 1994, when the first manual distress survey was reported for the section. The longitudinal cracking on the section fluctuates throughout the pavement’s history, but ultimately decreases between 2010 and 2012. By 2015, 371 feet of longitudinal cracking is observed along the section. The decrease in cracking reported is likely a result of the construction event (CN=3) that took place on this section in 2012 during which some of the PCC slabs were replaced. It is also hypothesized that the initiation and propagation of cracking along this section is related to the significantly higher amounts of precipitation and freezing index reported when compared to the other two test sections.

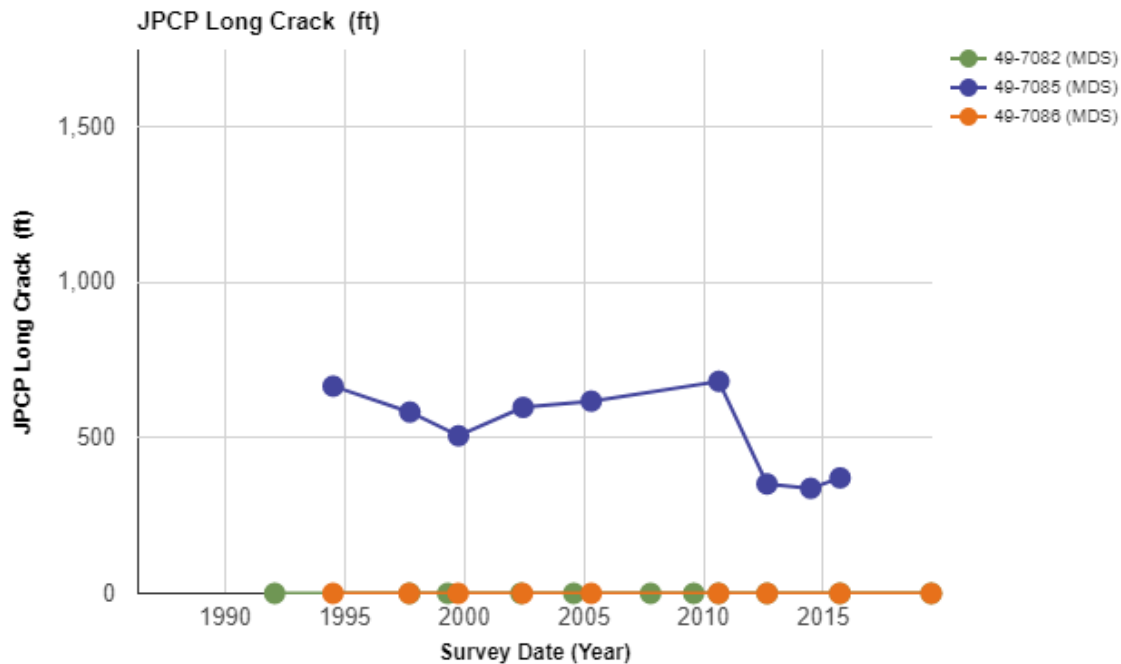


Figure 10. Time history of the length of NWP longitudinal cracks.

Transverse Cracking

Data on transverse cracking was collected between 1992 and 2019 as shown in Figures 11 and 12. Similar to the reported longitudinal cracking, substantial amounts of transverse cracking were only reported on section 49_7085, likely due to significantly higher amounts of precipitation and higher freezing index reported on this section as compared to the other two test sections. Transverse cracking reported on section 49_7085 was first reported in 1994, when 100 feet (14 cracks) were observed. The amount of cracking reported increased until 1997 and then subsequently decreased in 1999. However, the amount of cracking observed increased again between 1999 and 2010. The transverse cracking reported increased from 66 feet (10 cracks) in 1999 to 260 feet of cracking (47 cracks) in 2010, propagating at a rate of 17.6 feet/year over this 11-year period. In 2012, following the replacement of some of the PCC slabs during CN=3, the transverse cracking observed on section 49_7085 decreased to 189 feet (42 cracks). During the

last distress survey taken at this section in 2015, 2017 feet (42 cracks) were observed. For section 49_7082, transverse cracking was not observed on the section until 2007, 17 years after CN=1, when 6 feet (2 cracks) were observed on the section. The amount of transverse cracking slightly increased and by 2019, 15 feet (3 cracks) were observed. Therefore, cracking propagated at a rate of less than 1 foot/year over the 12-year period. No transverse cracking was reported on section 49_7086. No transverse cracking was reported on section 49_7086.

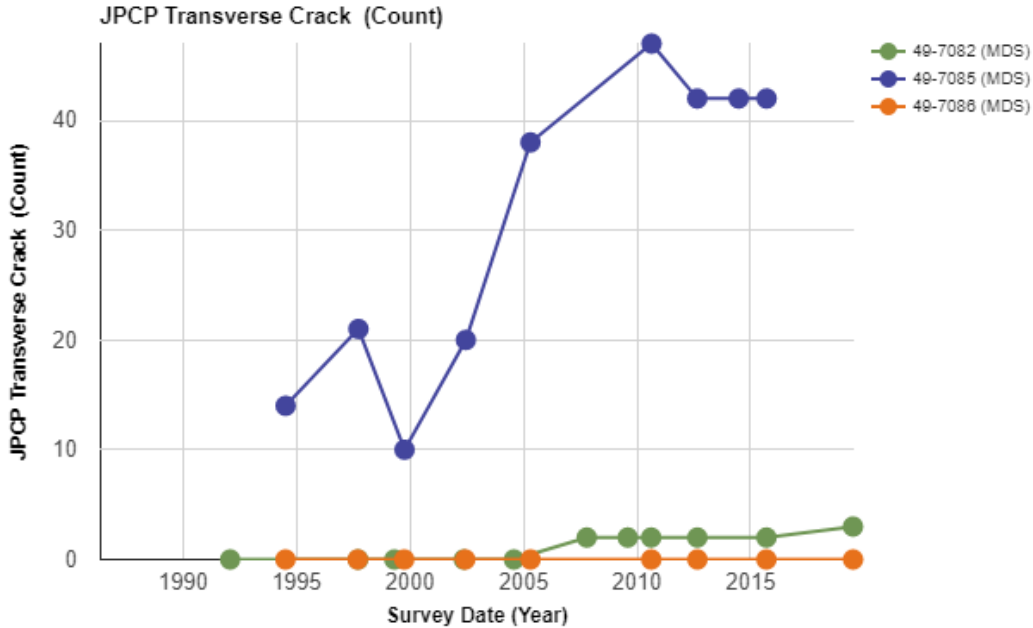


Figure 11. Time history of the number of transverse cracks.

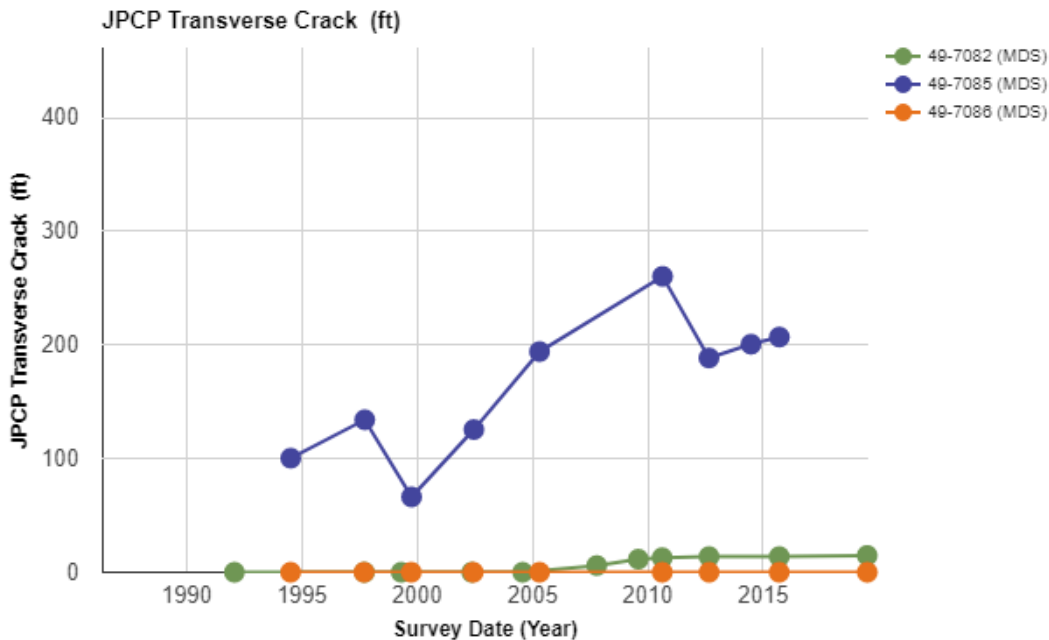


Figure 12. Time history of the length of transverse cracking.

Patching

Data on rigid patching was collected between 1992 and 2019 as shown in Figures 13 and 14. The only section where substantial rigid patching was reported is 49_7085. Rigid patching was first observed on section 49_7085 in 2012 when 1927.10 ft² (20 patches) were recorded the section. The amount of patching slightly increased between 2012 and 2015, and by 2015, 1,944 ft² of rigid patching was observed. Minimal rigid patching was observed on section 49_7086 starting in 2012, when 4 ft² of patching (3 patches) was recorded. The amount of patching observed slightly increased between 2012 and 2015 when 5 ft² of patching was observed. No rigid patching was observed on section 49_7082.

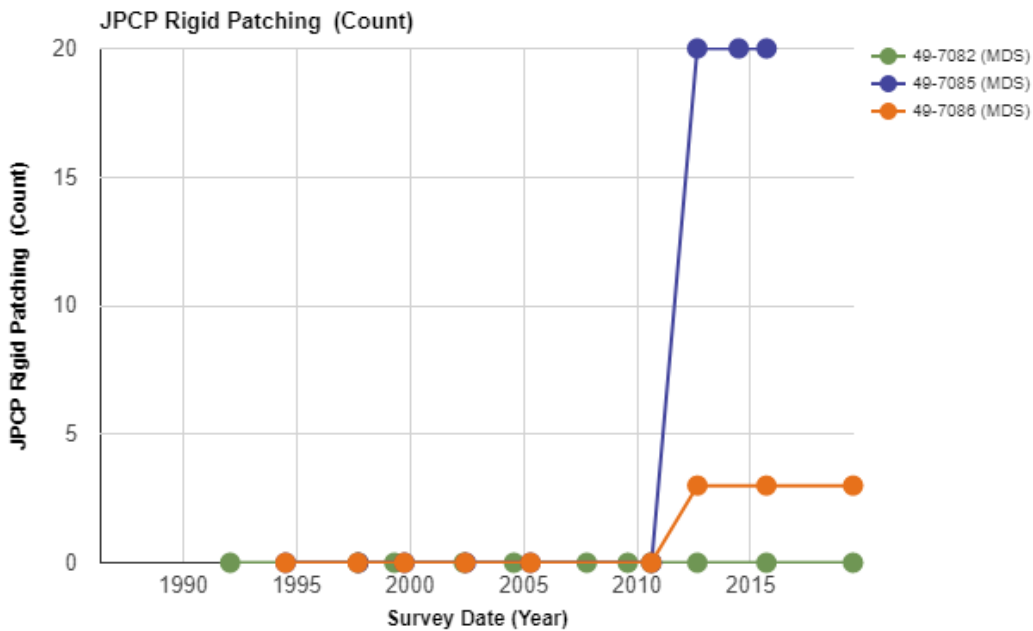


Figure 13. Time history of the number of rigid patches.

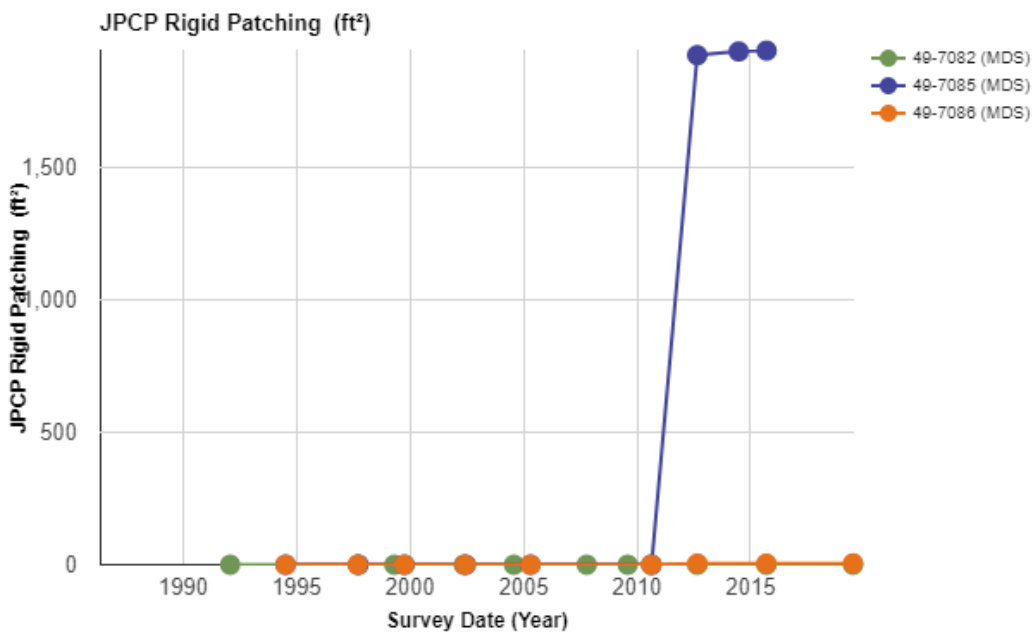


Figure 14. Time history of the area of patching.

Corner Breaks

Data on corner breaks was collected between 1992 and 2019 as shown in Figure 15. The only section where substantial corner breaks were reported is 49_7085. A corner break was first observed on section 49_7085 in 1994 when one corner break was observed on the section. An additional corner break was observed in 2012, resulting in a total of two corner breaks on this section. No corner breaks were observed on sections 49_7082 or 49_7086.

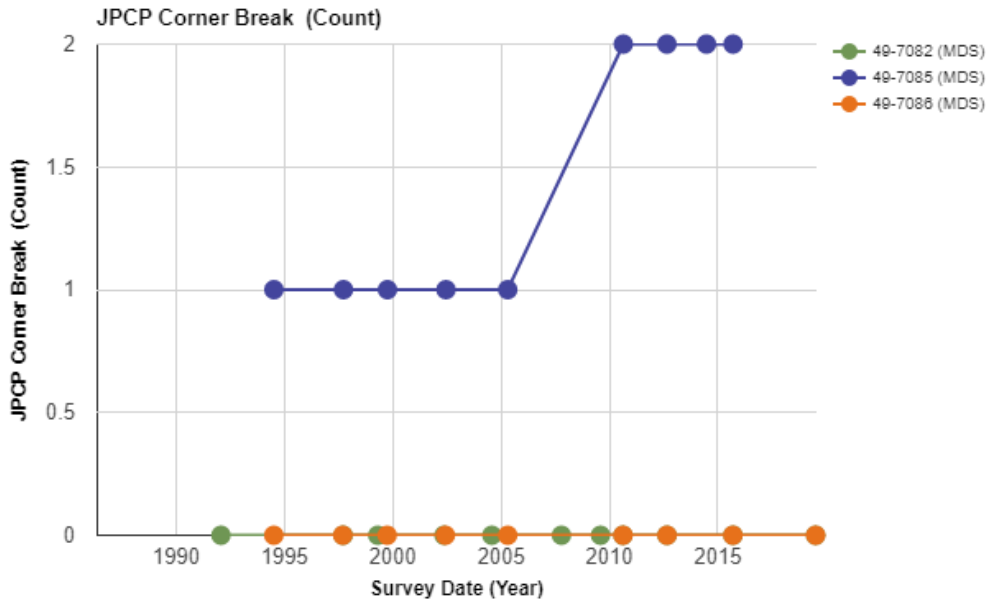


Figure 15. Time history of the number of corner breaks.

IRI

The average IRI measurements for the sections over time are shown in Figure 16. Section 49_7082 reported the lowest IRI of the three test sections between 1991 and 2019. The IRI on the section increased from 58 in/mi in 1991 to 100 in/mi in 2012, which means the performance of the pavement could be classified as “Good” to “Fair” based on FHWA performance definitions. In 2013, after the surface was diamond grinded, the IRI decreased and by 2014, the IRI on the section was 69 in/mi. The IRI on section 49_7082 remained relatively consistent between 2014 and 2019 when 63 in/mi of IRI was reported on the section.

Section 49_7085 had the next lowest amount of IRI reported throughout time. In 1993, IRI was reported to be 90 in/mi. IRI increased between 1993 and 2010 when IRI was reported as 151 in/mi. The pavement’s IRI performance during this time is classified as “Fair” based on FHWA performance definitions. Following the replacement of some of the concrete slabs and grinding of the surface in 2012, the section’s IRI decreased significantly to 112 in/mi. By 2016, the date of the last measurement for this section, the reported IRI had further decreased to 107 in/mi, but no construction or other event had been reported that would help explain this decrease. Section 49_7086 had the highest amount of IRI reported throughout time. In 1993, IRI was reported to be 90 in/mi. IRI increased between 1993 and 2010 when IRI was reported as 228 in/mi. The pavement’s IRI performance during this time is classified as “Fair” to “Poor” based on FHWA performance definitions. Following grinding of the surface in 2010, the section’s IRI decreased to 75 in/mi in 2012. By 2019, the date of the most recent measurement for this section, IRI was reported as 142 in/mi.

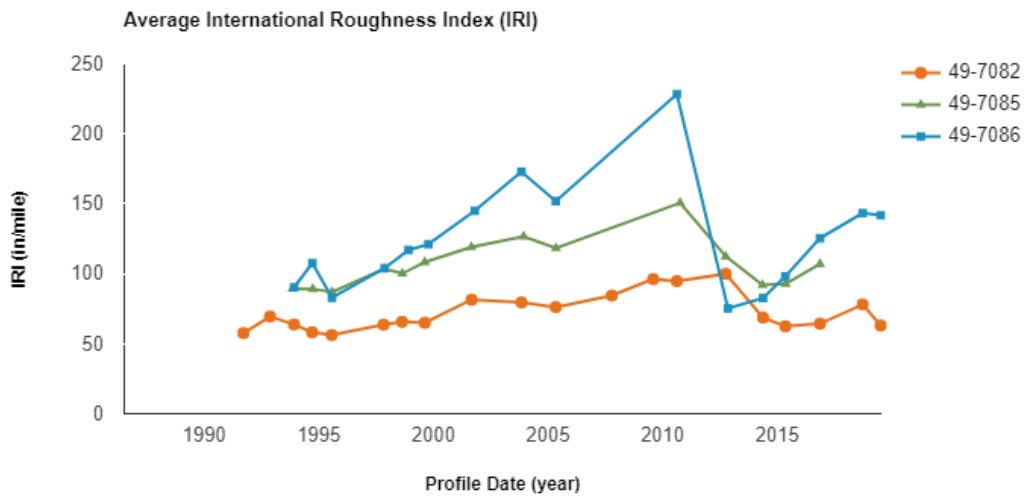


Figure 16. Time history plot of pavement roughness.

Faulting

The average faulting observed over time on the test sections is shown in Figure 17. Faulting on section 49_7082 fluctuated between the first time it was reported in 1992 and 2013. In 1990, faulting on the section was reported to be 0 in. By 2013, the reported faulting was 0.07 in. Following the preservation treatments in 2013 (diamond grinding and joint load transfer restoration) the faulting dropped to 0 in in 2015. By 2019, the faulting observed increases to 0.03 in. Faulting on test section 49_7085 increased between 1997, when faulting is first reported for this section, and 2010. In 1990, faulting on the section was reported to be 0.02 in. By 2010, the reported faulting was 0.09 in. Following CN=3, where the section received additional crack sealing and transverse joint sealing, the surface was diamond grinded, joint load transfer restored, and there was a replacement of some of the PCC slabs, the faulting observed on the site dropped to 0 in. The faulting on this section remained 0 in until the section went out of study. Faulting on section 49_7086 increased between the first time it was reported in 1997 and 2010. In 1997, faulting on the section was reported to be 0.01 in. By 2010, the reported faulting was 0.14 in. Following the preservation treatments in 2010 (surface grinding and partial depth patching) the faulting dropped to 0 in in 2012. However, the faulting observed increased immediately after and by 2019, the faulting reported was 0.11 in. Overall, section 49_7086 reported the highest average faulting and it is hypothesized this may be associated with the temperature regime.

As indicated earlier in the memorandum, test section 49_7086 had the largest amount of faulting and also the highest average annual air temperature at 48.4°F. Test section 49_7082 has the next highest amount of faulting and also the second highest average annual air temperature at 44.8°F, while test section 49_7085 had the lowest amount of faulting and also the lowest average annual air temperature at 39.5°F.

Wheelpath Surface Wear

The wheelpath surface wear observed over time on the test sections is shown in Figure 18. Prior to 2005, all three sections reported wheelpath surface wear of 0.12 in. Following 2005, the wheelpath surface wear depths reported increased for 49_7085 and 49_7086. In 2015, section 49_7085 reported 0.24-inch rut depth and section 49_7086 reported 0.2 in rut depth. Wheelpath surface wear is likely related to winter traffic—chains and studded tires—and is therefore greater on section 49_7085, which reported higher amounts of precipitation and is more likely to have traffic using chains and studded tires.

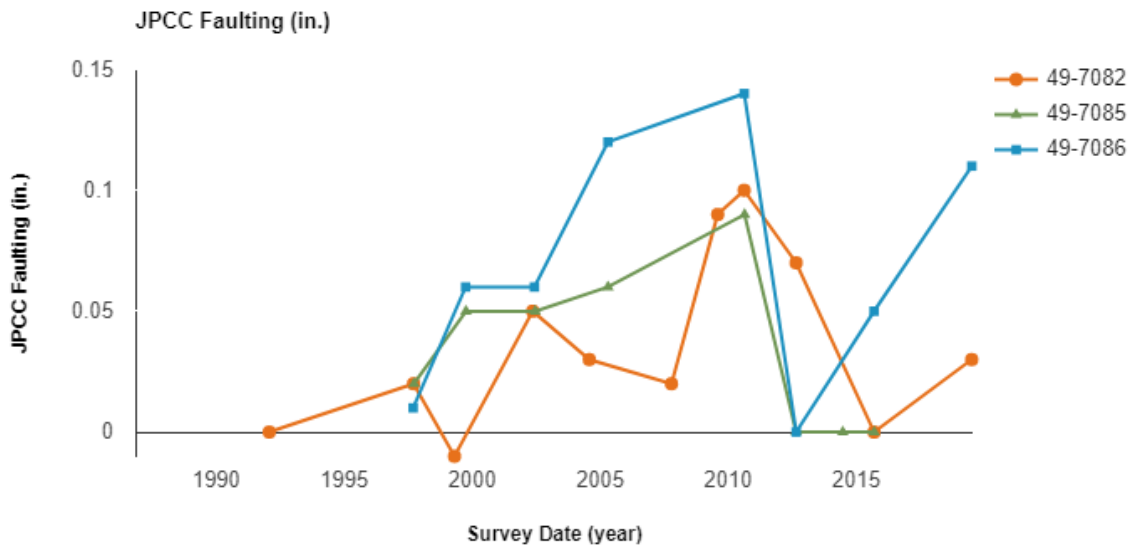


Figure 17. Time history plot of faulting.

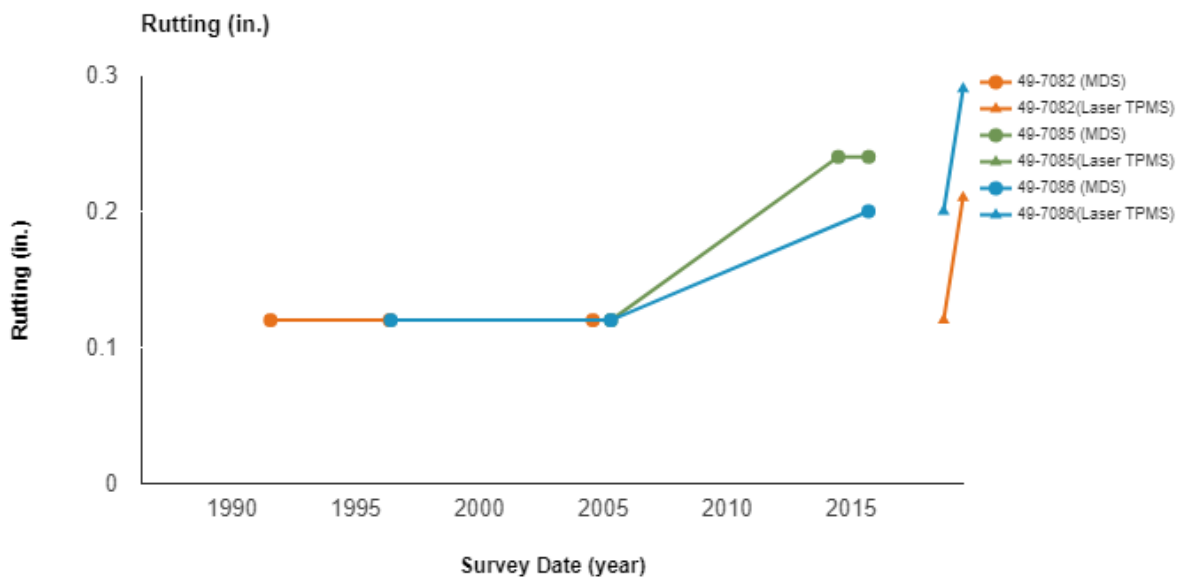


Figure 18. Time history plot of average wheelpath surface wear.

SUMMARY OF FINDINGS

LTPP test section 49_7082 is located on Interstate 15, northbound, in Box Elder County, Utah. Interstate 15 is a rural principal arterial-interstate with two lanes in the direction of traffic. Test section 49_7082 was accepted into the LTPP Program as part of the GPS-3 experiment in October 1989 with the knowledge it would officially start being monitored following the planned reconstruction completed in November 1990. The next construction event occurred in June 2013 when the surface was diamond grinded, and joint load transfer restored.

LTPP test section 49_7085 is located on U.S. 40, eastbound, in Wasatch County, Utah. U.S. 40 is a rural principal arterial with two lanes in the direction of traffic. Test section 49_7085 was accepted into the LTPP Program as part of the GPS-3 experiment in June 1991 with the knowledge it would officially start being monitored following the planned reconstruction completed in October 1991. The next construction event occurred in June 2001 when the section received crack sealing, transverse joint sealing, and lane shoulder longitudinal joint sealing (CN=2). A third construction event (CN=3) occurred in 2012 when the section received additional crack sealing and transverse joint sealing, the surface was diamond grinded, joint load transfer restored, and there was a replacement of some of the PCC slabs.

LTPP test section 49_7086 is located on State Route 154, southbound in Salt Lake County, Utah. State Route 154 is an urban principal arterial with three lanes in the direction of traffic. Test section 49_7086 was accepted into the LTPP Program as part of the GPS-3 experiment in June 1991 with the knowledge it would officially start being monitored following the planned reconstruction completed in October 1991. The next construction event occurred in May 2001 when the section received transverse joint sealing and lane shoulder longitudinal joint sealing (CN=2). A third construction event (CN=3) occurred in 2010 when the section received surface grinding and partial depth patching. A final event (CN=4) occurred in 2013 when the test section surface was diamond grinded and additional transverse joint sealing occurred.

A summary of the performance factors and metrics for the three test sections are provided in Table 5. In the case of the metrics, the green fields indicates attributes that should positively affect the performance of test section when compared to the other sections, and the red indicates attributes that should negatively affect the test section when compared to the other sections. Yellow indicates the attribute should not strongly affect the test section as the value reported for the section is between the values reported for the other two sections. Similarly, for the case of the metrics, greens indicates a test section with a better performance, while red indicates a test section with worse performance. Yellow indicates the performance of the test section is in between the performance of the other test sections.

Based on the results summarized in Table 5, test section 49_7085 appears to have performed the worst of the three test sections for most performance metrics. This seems to be largely attributed to two of the climatic factors reported at this test section (annual precipitation and freezing index), which were notably higher than the other test sections. These factors likely contributed to higher amounts transverse cracking and patching. Test sections 49_7082 and 49_7086 overall reported similar performance. However, the faulting on test section 49_7086 was notably worse than section 49_7082, which resulted in higher IRI on test section 49_7086. It is hypothesized the higher amount of faulting is due to higher temperatures at test section 49_7096, but it could also be related to other factors such as ambient conditions at the time the test section was constructed, temperature conditions at the time faulting and IRI measurements were made (i.e., warping and curling of the slabs, etc.).

In summary, the performance of a pavement is driven by the separate and combined effect of the following four factors:

- Traffic (loadings and volumes),
- Environmental conditions (i.e., surface and subsurface moisture and temperature),
- Pavement structure (layer thicknesses and strengths, construction quality, etc.), and
- Subgrade soil (strength, depth to bedrock, etc.).

Table 5. Summary of Performance Factors and Metrics

Performance Factors	Test Section 49_7082	Test Section 49_7085	Test Section 49_7086
Average Annual Precipitation, in	19.6	36.4	18.3
Average Freeze Index, °F °day	1,038	1,605	667
Average Annual Air Temperature	44.8°F	39.5°F	48.4°F
Cumulative ESALs	18,646,159	7,501,354	5,145,025
Max PCC Layer Modulus (Field), ksi	9,598	7,409	8,021
Max PCC Layer Modulus (Laboratory), ksi	5,400	4,100	4,100
PCC Layer Thickness, in	9.8	9.8	10.1
Performance Metrics			
Max. Measured Deflection, mils	4.6	7.7	5.4
Max Longitudinal Cracking Value, ft	0	681	0
Max Transverse Cracking Value (count)	3	47	0
Max Transverse Cracking Value (length, ft)	15	260	0
Max Patching Value (count)	0	20	3
Max Patching Value (area, ft ²)	0	1,944	5
Max Corner Breaks	0	2	0
Max Average IRI Value, in/mile	100	151	228
Max Faulting Value, in	0.10	0.09	0.14
Wheelpath surface wear, in	0.12	0.24	0.2

Based on this desktop study, it appears that differences in the performance of the three sections was largely driven by environmental factors, while the remaining factors do not appear to have contributed to the differences. Test section 49_7085 had the worst performance in terms of longitudinal cracking, transverse patching, corner breaks, and wheelpath surface wear, and this performance appears to be driven by the significantly higher precipitation and freezing index at the site. While test section 49_7086 had the worst faulting and IRI, with higher temperatures apparently driving the higher faulting levels, which in turn affected the IRI values.

FORENSIC EVALUATION RECOMMENDATIONS

Based on the information gathered and analyzed in this desktop study, the following follow-up actions are recommended:

1. Perform at least one more round of performance monitoring on test sections 49_7082 and 49_7086, including manual distress surveys, longitudinal and transverse profile surveys, and deflection testing. (Note: test section 49_7085 was taken out of study in 2017, but it was included in this study for comparison purposes).
2. Within test section coring, once the sections are ready to be taken out-of-study to:
 - a. Confirm the layer thicknesses match those reported when the test section was incorporated into the LTPP program.
 - b. Identify key properties of the base and subgrade layers via materials sampling and field and laboratory testing.
3. Clarification and exploration as to why section 49_7085 is labelled as a Dry climate site in the LTPP database even though the reported precipitation at this section indicates it is a Wet climate site.
4. Further pursue reason(s) for higher faulting and IRI at test section 49_7086, including review of climatic conditions at the time of construction as well as review of faulting and IRI surveys results relative to climatic conditions.

It is anticipated the above follow-up recommendations will be accomplished through a joint effort involving the Utah DOT, the FHWA LTPP program (including Data Collection Contractor), and the TPF-5(332) project team.

ADDENDUM: FOLLOW-UP INVESTIGATION OF TEST SECTIONS 49_70**

After completing the desktop study, the resulting technical memorandum was provided to industry and Agency personnel familiar with test sections 49_7082, 49_7085, and 49_7086. These personnel noticed discrepancies between the construction events reported in InfoPave™ and the actual work done on test sections 49_7082 and 49_7086. While the construction events described in the original memorandum (September 3, 2020) reflect what was reported in InfoPave™ at the time the memorandum was prepared, the actual construction events carried out by Utah DOT on test sections 49_7082 and 49_7086 deviated from what was reported. Therefore, to reconcile these differences, the construction events were updated based on the construction events documented on the test sections, which were provided by the Utah DOT LTPP Coordinator. Additionally, the climate classification methodology for the test sections was also investigated. As noted in the original memorandum, precipitation for test section 49_7085 falls outside the “Dry” definition (20 inches per year) used for classifying the climate of a site. This follow-up study investigates the discrepancy between the climate classification of the test section and the actual precipitation reported on the section over time. In this addendum, the specific changes and clarifications made to the LTPP database³ and the effects of these changes on the initial analysis conducted as a part of the desktop study are summarized.

Pavement Structure and Construction History

As discussed, further investigation of the test sections revealed differences between the construction events reported in InfoPave™ and the actual construction events that occurred. Using DOT and industry knowledge and documentation on each test section, revisions to the LTPP database were made. Table 5 summarizes these changes.

At the time desktop study was prepared, test section 49_7082 reported two construction events—the initial incorporation of the test section into the LTPP program in October 1989 (CN=1) and diamond grinding and joint load transfer in June 2013 (CN=2). However, further investigation revealed additional work was carried out on the test section in June 2013 that was not captured in the LTPP database. In addition to the grinding and joint load transfer reported on the section during CN=2, transverse joint sealing and lane-shoulder longitudinal joint sealing also took place.

Test section 49_7086 reported four construction events in InfoPave™—the initial incorporation of the test section into the LTPP program in June 1991 (CN=1), transverse and shoulder longitudinal joint sealing in May 2001 (CN=2), partial depth patching outside the joints and grinding in November 2010 (CN=3), and joint sealing and diamond grinding in June 2013 (CN=4). However, changes had to be made to the events reported in InfoPave™ for CN=3 and CN=4, as the actual construction events on the test section deviated from the ones reported. For CN=3, it was found that partial depth patching at locations other than the joints did not occur on the test section in November 2010. Instead, the test section received transverse joint sealing, full depth transverse joint repair, and partial depth patching at the joints in addition to the grinding originally reported on the test section during CN=3. InfoPave™ also reported a fourth construction event (CN=4) on the test section, which included joint sealing and grinding in June 2013. However, based on knowledge and documentation provided by Utah DOT staff, this construction did not occur and therefore was removed from the LTPP database.

³ While changes have been made to the LTPP database, the changes will not be reflected in InfoPave™ until the next Standard Data Release (SDR) in 2021.

Table 5. Changes to CN events for test sections 49_7082 and 49_7086

Section	CN	CN Assign Date	CN Change Reason Prior to Update	Updates	Final CN Change Reasons
497082	1	10/31/1989		No change.	
	2	6/1/2013	12 - Grinding and 50 - Joint Load Transfer Restoration	Added CN_CHANGE_REASON 2 - Transverse Joint Sealing and 3 - Lane-Shoulder Longitudinal Joint Sealing.	2, 3, 12, 50
497086	1	6/7/1991		No change.	
	2	5/1/2001	2 - Transverse Joint Sealing and 3 - Lane-Shoulder Longitudinal Joint Sealing	No change.	2, 3
	3	11/20/2010	6 - Partial Depth Patching of PCC Pavement Other Than at Joint and 12 - Grinding	Removed CN_CHANGE_REASON 6 and added CN_CHANGE_REASON 2 - Transverse Joint Sealing, 4 - Full Depth Transverse Joint Repair patch and 54 - Partial Depth Patching of PCC Pavements at Joints.	2, 4, 12, 54
	4	6/1/2013	2 - Joint Sealing and 12 - Grinding	CN 4 Removed.	CN removed.

Pavement Distress History

Based on the changes made to the construction history of test sections 49_7082 and 49_7086, the pavement distress history, discussed in the desktop study, was reassessed. A summary of the major additions and changes to the original (September 3, 2020) memorandum are summarized below.

IRI

While the memorandum provides an accurate summary of the changes in IRI over time for each test section, the updated construction history of test section 49_7086 helps better explain the changes in IRI reported for that section. Under the previous assumptions that the test section was grinded during a fourth construction event (CN=4) in June 2013, it would have been expected that IRI following this event would decrease. However, as depicted in Figure 16, a significant decrease in the average IRI reported occurs after the third construction event in 2010, but not in 2013 after the “supposed” fourth construction event. As no construction event (and therefore, no surface grinding) took place in 2013, it is reasonable for the IRI reported on the test section continued to increase after CN=3.

Faulting

Like IRI, the findings on faulting reported in the original memorandum already provide an accurate summary of the history of faulting for the three test sections. The updated construction history of the test sections does, however, better explain the faulting observed over time. Specifically, for test section 49_7086, the continual increase in faulting between 2013 and 2019 is more aligned with the updated construction history of the test section. While previously, under the assumption that a fourth construction

event of joint sealing and grinding took place in June 2013, the increase in faulting in 2015 was counterintuitive; diamond grinding is a technique that helps mitigate faulting along joints. However, as no grinding occurred in 2013, the trend shown in Figure 17 seems more reasonable.

Climate History

As noted in the original memorandum and as depicted in Figure 6, while test section 49_7085 reports high levels of precipitation each year, the test section was classified as being a “Dry” region. Further information as to why the test section was classified as “Dry,” given the precipitation reported on the section, was pursued. In the current LTPP dataset, it appears climate classifications are based on the location of the section rather than the average annual precipitation or freezing index at the test site. However, starting with the 2021 LTPP data release, the climatic region for each LTPP test section will be assigned using the MERRA-2 dataset. In the updated web portal, the average annual freezing index and precipitation will be used to classify the climatic region of each test section. Through this update, the threshold between Wet and Dry regions will be an average annual precipitation of 508 millimeters (20 inches). Therefore, test section 49_7085 will be classified as being in a “Wet” region based on these conditions.

SUMMARY

This addendum focused on identifying, correcting, and explaining the construction history and climate classification of the test sections analyzed in the initial memorandum. Based on the knowledge and documentation of Utah DOT staff, industry, and regional contractors, it was found the actual construction history of test sections 49_7082 and 49_7086 deviated from what was reported in the LTPP database and was updated accordingly. The updated construction history helped better explain the performance of test section 49_7086—particularly with regards to the IRI and faulting observed on the section over time. Additionally, further information on why test section 49_7085 was classified as “Dry,” given the precipitation reported on the section, was pursued. It was found that in the current LTPP dataset, climate classifications are based on the location of the section rather than the average annual precipitation or freezing index at the test site. However, starting with the 2021 LTPP data release, an updated climate classification methodology, which will use the average annual precipitation of a test section, will be implemented. Using the new classification methodology, test section 49_7085 will be classified as being in a “Wet” region.